EAO.3 Microwave/Optical Studies of Saline Ice, Snow, Melt Ponds and Refrozen Melt Pond Ice

J. Bredow
D. Gibbs
C. Betty
A.K. Fung

University of Texas at Arlington
PO Box 19016
Arlington, TX 76019
Phone: (817)-273-3497
FAX: (817)-273-2253

S.P. Gogineni

University of Kansas
2291 Irving Hill Rd.
Lawrence, KS 66045

ABSTRACT

Optical and microwave measurements of a variety of ice and snow targets were obtained in a large indoor cold room at the U.S. Army Cold Regions Research and Engineering Laboratory (CRREL) in Hanover, N.H. Bistatic measurements performed in the plane of incidence were obtained at 632.8 nm and backscatter measurements as a function of incidence angle were obtained at 13.6 GHz. The 632.8 instrument that was used is a portable version of the UTA Automated Bidirectional Reflectance Acquisition Measurement System (ABRAMS) and the University of Kansas 13 GHz instrument is a step frequency radar that is based around the HP8753 network analyzer. In this report we will consider the scattering behavior of thermally modified saline ice, snow, melt ponds and refrozen melt pond ice. Preliminary results indicate that air bubbles in saline ice and melt pond ice are important sources of scattering at optical wavelengths. Microwave frequencies, on the other hand, are sensitive to brine inclusions in the ice and to liquid water at the ice surface; microwave measurements showed a dramatic (8 dB) decrease in nadir backscattering as a quiescent melt pond refroze. Other topics that will be included in this report deal with system calibration, and the use of polarization in the plane of incidence to distinguish between volume and surface scattering.

1. Introduction

Saline ice growth was begun on January 14, 1992, in an indoor cold room at the U.S. Army Cold Regions Research and Engineering Laboratory (CRREL) in Hanover, New Hampshire. The 5 m x 6 m, by 1 m deep sheet of saline ice was grown from water of approximately 23 ppt by weight of sea salt. Located 20 cm above the center of the ice were two I-beams, spaced 1 m apart, which provided for two 2 m x 6 m areas, at each end of the ice sheet to conduct experiments. After the initial ice growth phase was completed on January 19, 1992, this ice sheet had a bulk salinity of 6.7 ppt. The ice consisted of a 0.5 to 1 cm layer of 1 to 3-mm diameter randomly oriented crystals overlying a 15-cm thick layer of congelation ice with crystalline c-axes predominantly horizontal in orientation. From mid-January to mid-February the cold room temperature was cycled from near-0^{O}F to about 28^{O}F to simulate natural diurnal temperature variations. By mid-February the bulk salinity had dropped to a few ppt and the structure of the congelation ice was considerably modified. The platelet structure of the congelation ice crystals was no longer apparent in the ice vertical thin sections due to leakage of brine at near-freezing temperatures, and the edges of the large congelation ice crystals were rounded as a result of the thermal modification. The same temperature cycles were then repeated until mid-March when extreme temperature forcing was performed. In mid-March, prior to undertaking measurements, temperatures were elevated to 60^{O}+F for several hours, and the appearance of the ice

changed as follows: as the surface of the ice reached about 30°F the ice whitened considerably as a result of the brine drainage from the upper layer of the ice. Further temperature forcing resulted in the formation of 1 to 2-cm deep melt pond as a result of melting of the ice surface. Subsequently, the cold room temperature was reduced to 0°F for several hours until the melt pond had frozen; this completed the thermal modifications of the ice.

Structurally this last sheet consisted of a 1 to 2-cm thick layer of very low salinity ice (i.e., the frozen melt pond) overlying the thermally-modified saline ice. The former appeared to be nearly transparent, containing about 5% by volume fraction of 1-mm diameter air bubbles. Near the interface with the thermally modified ice a much higher volume fraction of similarly sized air bubbles was present, apparently having been trapped as the melt pond froze. The surface of the frozen melt pond had an estimated correlation length of 3 cm, an rms height of less than 0.5 mm, and did not appear to have a gaussian distribution. The overall thickness of this ice sheet was about 28 cm.

During the same interval of experiments described above, a 9-cm deep layer of natural snow, which was piled on a relatively small portion of the ice sheet, experienced the same temperature cycling as the ice sheet. Initially the snow particles (i..e, ice crystals) were less than 1 mm diameter. The estimated volume fraction for this snow layer at the time of the measurements was 40%. Measurements were performed throughout the temperature cycling.

2.0 Optical Results

An example of the results obtained with the 632.8 nm system is shown in Fig. 1. Here we show σ^o for a source incident angle of 0° and as a function of receive angle for the saline ice. Notice that a strong specular peak occurs for like-polarization, indicating the importance of surface scattering. When the receiver was shifted away from the specular direction the like- and cross-polarization levels dropped dramatically but were of about equal magnitude. Although the scattering away from specular was weak (at least weak when compared to the Lambertian calibration standard), the equal magnitudes of like- and cross-polarization for scattering in the plane of incidence tells us that multiple-scattering (i.e., volume scattering) is the most important scattering mechanism for scattering away from the specular direction. Note that measurements were performed for other transmitter angles (with scanning of the receiver in the plane of incidence), however the results pointed to the same scattering mechanisms. Note that the gaps in Figs. 1 and 2 are due to angular regions where the automated instrument was unable to obtain data.

From the ice physical characteristics data that is available we believe that the primary volume scattering contribution was from air pockets within the ice. Saline ice consists of randomly oriented crystals, brine inclusions and air pockets: the strongest electrical discontinuity for optical wavelengths occurs between air and ice; ice, brine and air having refractive indices of 1.31, 1.33-1.35 and 1.0, respectively. Since the volume fractions of air and brine in the ice were roughly equal, we believe that the air pockets were the major scattering contributors.

The predominant scattering mechanism of snow is a different matter. When the snow was illuminated with the laser a bright red glow appeared within the ice. The measurements depicted in Fig. 2 are consistent with this description, showing no distinct specular effect for scattering from snow. This and the equal-magnitude levels of like- and cross-polarization in the plane of incidence point to volume scattering as the dominant scattering mechanism for snow. This is also supported by statements of the previous paragraph, considering that dry snow is a mixture of ice crystals and air.

3.0 Microwave results

The angular scan of backscattering coefficient versus angle was dominated by surface scattering except at higher incidence angles where scattering from brine inclusions was weak but apparent. The same basic results were obtained of the refrozen melt pond ice. The most interesting result of the microwave measurements was of the metamorphosis of the scattering signature as the melt pond refroze. At normal incidence (nadir) especially dramatic changes occurred as the ice first began to form and then began to thicken (See Fig. 3). Notice that with open water the scattering was high and then dipped by over 20 dB as the ice grew to about 1 mm in thickness. As the ice continued to grow the scattering increased in strength to about its open water value and then dropped gradually to about 8 dB below that of the open water. The depicted variation is a result of interference between scattering from the ice surface and scattering from the surface of the water beneath the ice. Once the ice grows to a thickness of greater than 1 cm the loss in microwave propagation through the ice is

significant enough that reflection from the surface of the underlying water becomes insignificant relative to that from the surface of the ice.

4.0 Summary

The results indicate that surface scattering is an important scattering mechanism for saline ice and refrozen melt pond ice at both optical wavelengths and microwave frequencies. This is a result of the strong electrical discontinuity between air and ice: at 632.8 nm the refractive index of ice is about 1.3 as compared to 1.0 for air; and at 13 GHz the refractive index of ice is about 2 as compared to 1.0 for air. Volume scattering within the ice, on the other hand, is weak primarily due to the low volume fractions of brine and air in saline ice (or refrozen melt pond ice). Away from the specular direction volume scattering can be important if the ice surface is sufficiently smooth. In these cases it appears that air pockets within the ice are the most important volume scatterers at optical wavelengths, air and ice having a substantially larger electrical contrast than brine and ice. On the other hand brine pockets within the ice are the most important volume scatterers at microwave wavelengths, brine and ice having substantially larger electrical contrast than air and ice. For snow, volume scattering at optical wavelengths was strong and was the predominant scattering mechanism.

Microwaves are much more sensitive to the presence of liquid water than are optical sensors. This is due to the large refractive index of liquid water at microwave frequencies, i.e., nearly 8. The change in refractive index (at microwave frequencies) as water changes to ice was clearly evident in microwave measurements near nadir as the melt pond refroze: at 0^o incidence the backscattering level dropped by nearly 10 dB as the ice froze.

The results discussed in this paper point to the potential usefulness of multispectral (microwave/optical) studies of sea ice.

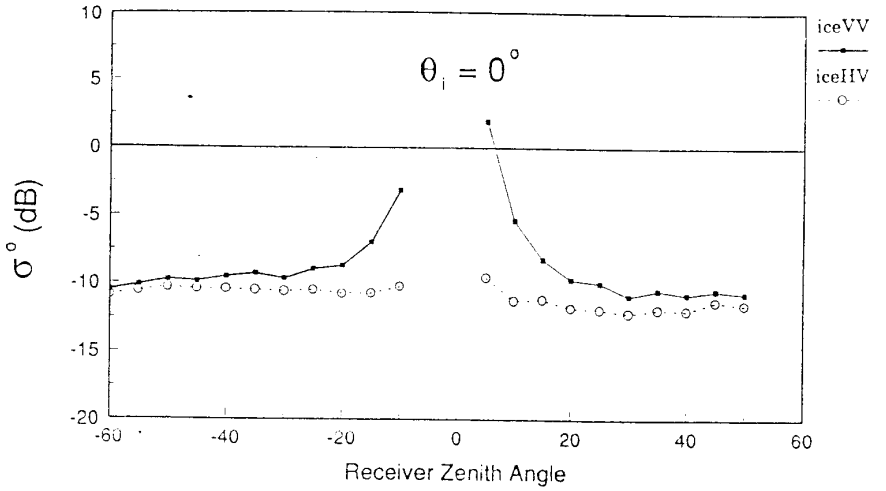

Figure 1: σ^o for a source incident angle of $\theta_i = 0^o$ of the saline ice.

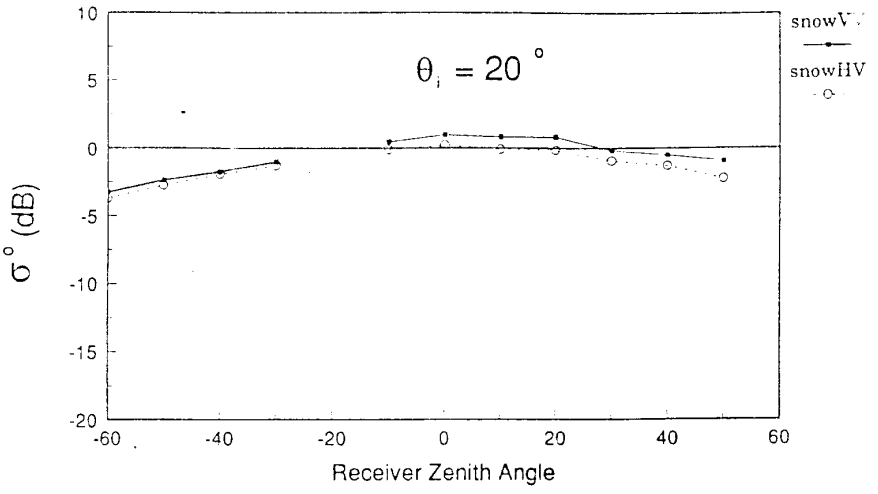

Figure 2: σ^{o} of the snow for a source incident angle of $\theta_i = 10^{o}$.

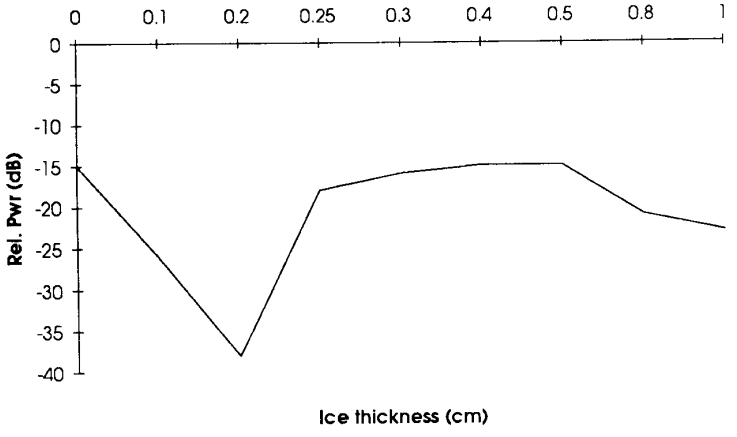

Figure 3: Microwave scattering from open water and then ice, as the ice grows to a thickness of about 1 cm.